# Supporting Information for

# Destruction of Per/poly-fluorinated Alkyl Substances by Magnetite Nanoparticle-Catalyzed UV-Fenton reaction

*Danielle. R. Schlesinger, Collin McDermott, Nam Q. Le, Jesse S. Ko, James K. Johnson, Plamen A. Demirev, Zhiyong Xia**

The Johns Hopkins University Applied Physics Laboratory, Laurel, MD 20723, USA

*Corresponding author: zhiyong.xia@jhuapl.edu

**This file includes the following content:**

**ST1.** Percent destruction of PFOA and PFOS with variable UV exposure time, hydrogen peroxide ($H_2O_2$) concentration, and $Fe_3O_4$ concentration.

| UV time (min) | $H_2O_2$ conc. (M) | $Fe_3O_4$ conc. (ppm) | % Destruction PFOA[a] | % Destruction PFOS[a] |
|---|---|---|---|---|
| 5 | 0.10 | 100 | 13.3 | 20.0 |
| 5 | 2.55 | 100 | 26.7 | 38.7 |
| 5 | 2.55 | 1050 | 68.0 | 88.0 |
| 5 | 2.55 | 2000 | 66.7 | 84.7 |
| 5 | 5.00 | 1050 | 56.0 | 75.3 |
| 5 | 5.00 | 2000 | 68.7 | 83.3 |
| 32.5 | 0.10 | 1050 | 6.7 | 36.0 |
| 32.5 | 0.10 | 2000 | 0.0 | 33.3 |
| 32.5 | 2.55 | 100 | 67.3 | 76.0 |
| 32.5 | 2.55 | 1050 | 61.3 | 86.0 |
| 32.5 | 2.55 | 2000 | 66.0 | 80.7 |
| 32.5 | 5.00 | 100 | 74.7 | 74.0 |
| 32.5 | 5.00 | 2000 | 69.3 | 82.7 |
| 60 | 0.10 | 1050 | 0.0 | 33.3 |
| 60 | 0.10 | 2000 | 6.7 | 34.0 |
| 60 | 2.55 | 100 | 65.3 | 78.7 |
| 60 | 2.55 | 2000 | 63.3 | 74.0 |
| 60 | 5.00 | 100 | 39.3 | 64.7 |
| 60 | 5.00 | 1050 | 13.3 | 47.3 |
| 60 | 5.00 | 2000 | 54.0 | 72.7 |

[a] Percent error for samples was calculated to be ±7.0% for PFOA and ±4.9% for PFOS.

## S1. High Resolution Mass Spectrometry (HRMS) Experimental Details.

HRMS analysis was conducted on a Thermo Scientific Orbitrap Exploris 240 instrument. Control PFOA and PFOS samples (100 ppm) and samples after reaction at specific conditions (pH 7 or pH 9, 2.5M or 5M) were analyzed under the same instrumental conditions. Samples were prepared by filtration through 0.2 µm PTFE syringe filters followed by dilution in methanol in a 1:10 ratio of sample to methanol. Sample solutions were introduced by continuous direct infusion (10 µl/min)

into the electrospray ion source of the instrument and were analyzed in both negative and positive ion modes. Optimized source conditions were 3600V and 2600V spray voltage for positive and negative ion generation, respectively. The instrument was autotuned (rf lens rel. value 70%) with automatic gain control and custom injection time functions switched on. The system was mass calibrated in both polarities each day before each analysis by following the manufacturer's protocols with calibration compound mixtures purchased from the manufacturer. The resolving power was set at 240,000 FWHM. For each analyzed sample, 150 individual ion spectra were collected in a range from 50 to 500 m/z (50 to 700 m/z for PFOS) in MS or tandem MS mode for either polarity, respectively. The estimated experimental mass accuracy was better than 5 ppm in the entire range. Tandem mass spectrometry was performed by isolating monoisotopic precursor ions (window 1 m/z) and subsequent manual optimization of the relative collision energy value for efficient collision-induced dissociation (CID). Elemental composition assignments from accurate mass determination of select ions in the averaged negative ion spectra were performed using the Web-based software Chem Calc (https://www.chemcalc.org/mf-finder). The mass of a single electron (0.00054 Da) was subtracted from each experimentally determined anion mass, i.e., the mass of the neutral species was input into the program. The calculated masses of the species with tentative elemental composition assignment were restricted to be less than 5 ppm than the measured neutral species mass.

**S2. XANES Experimental Details.**

$Fe_3O_4$ nanoparticles were filtered from solutions following Fenton reactions in the UV oven and collected on P5 grade filter paper. A section of filter paper approximately 1 cm × 2 cm with a uniform layer of magnetite was cut from the whole filter paper. The filtered $Fe_3O_4$ section was mounted between Kapton tape and X-ray clean polyfilm. Fe XANES were collected for each

sample from -100 to -20 eV below the Fe k-edge (5.0 eV step size), from -20 eV below to 50 eV above the Fe k-edge (0.2 eV step size), and 50 eV to 150 eV above the Fe k-edge (5.0 eV step size) with a 0.5 sec point$^{-1}$ acquisition time. Spectra were collected in both transmission and fluorescence modes, and a standard ionization chamber and a four element Silicon drift detector were used for each of these measurement types, respectively. Fe XANES standard spectra of $Fe_3O_4$, Fe foil, hematite ($Fe_2O_3$), and wustite (FeO) were collected and used to calibrate all samples to the same Fe K-edge energy and to conduct linear combination fitting of each spectrum.

## S3. Results of HRMS and XANES Analyses.

### S3.1. HRMS.

High resolution negative ion mass spectra of PFOS control and PFOS reacted under varying conditions are plotted on Figure SF1. For the control, the most intense ion peak corresponds to intact PFOS anion $\mathbf{[C_8F_{17}O_3S]^{-\cdot}}$ at m/z 498.93015 (molecular ion). The absolute intensity of the intact PFOS peak in spectra from reacted samples is decreasing considerably. Similar to PFOA, the initial PFOS sample has been completely degraded at 5M $H_2O_2$ and pH9, and no molecular ion is observed in the spectrum (Figure SF2.**C**). Additional peaks observed in spectra from reacted PFOA and PFOS are interpreted as the respectve degradation products (Supplementary Tables ST2 and ST3).

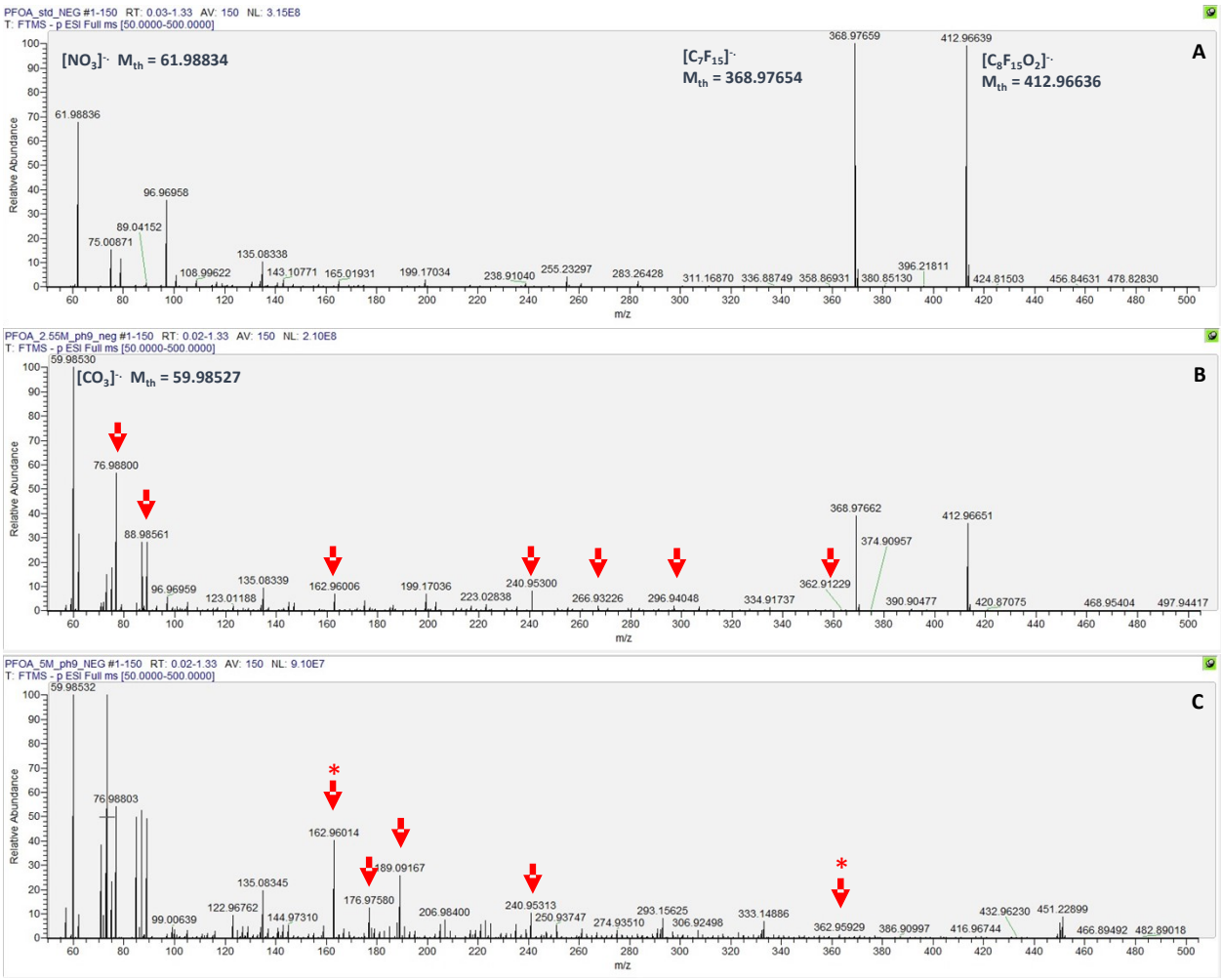


**Figure SF1**. Comparison between negative ion spectra of PFOA control (**A**) and PFOA reacted at different conditions: 2.55M $H_2O_2$ at pH9 (**B**), and 5M $H_2O_2$ at pH9 (**C**). Arrows indicate peaks corresponding to degradation products, asterisks indicate peaks reported in the literature.

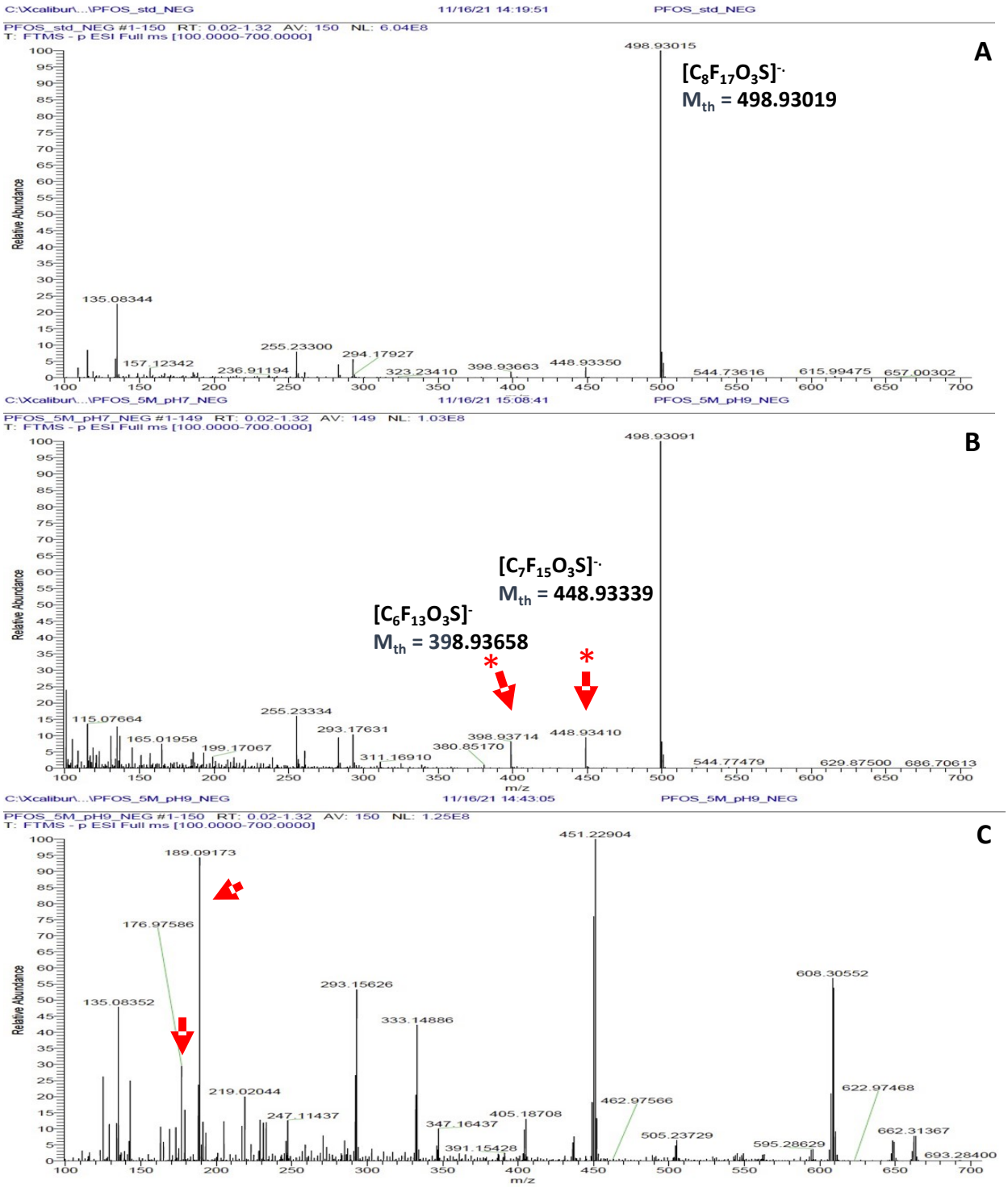


**Figure SF2**. Comparison between negative ion spectra of PFOS control (**A**), and PFOS reacted at different conditions - 5M $H_2O_2$ at pH7 (**B**), and 5M $H_2O_2$ at pH9 (**C**). Arrows indicate peaks corresponding to degradation products, asterisks indicate peaks reported in the literature.[2] Strong peaks in spectrum C (at m/z 293, 333, 405, 451, 608) are attributed to metalloorganic cluster anions, that are also observed in spectra of blank (non-PFOS-containing) samples at the same experimental conditions.

## S3.2. FLUORESCENCE PROBE MEASUREMENTS.

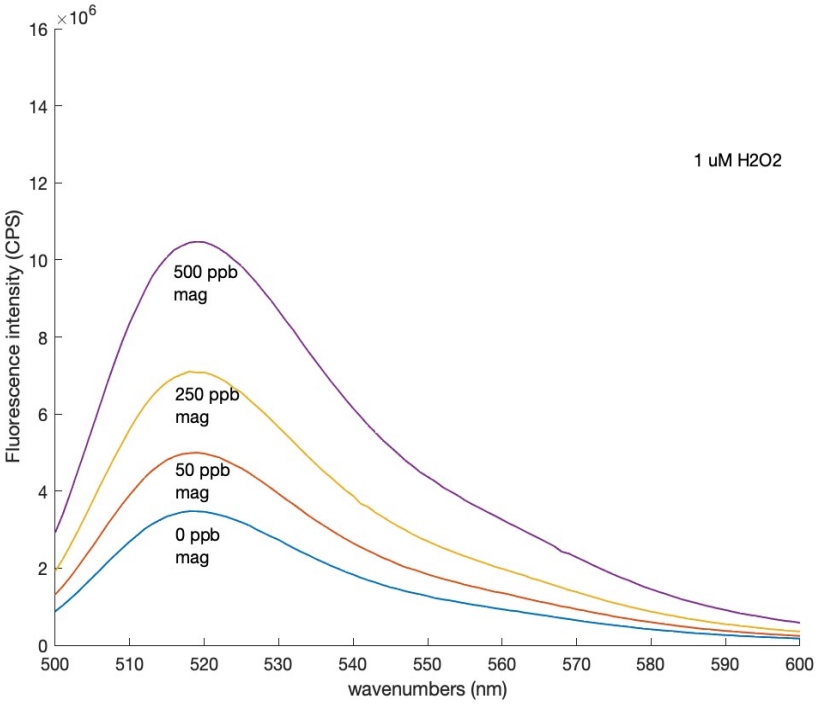


**Figure SF3.** Fluorescence intensity of detected ROS with increasing concentration of $Fe_3O_4$ nanoparticles.

## S3.3. MAGNETITE ADSORPTION CONTROLS

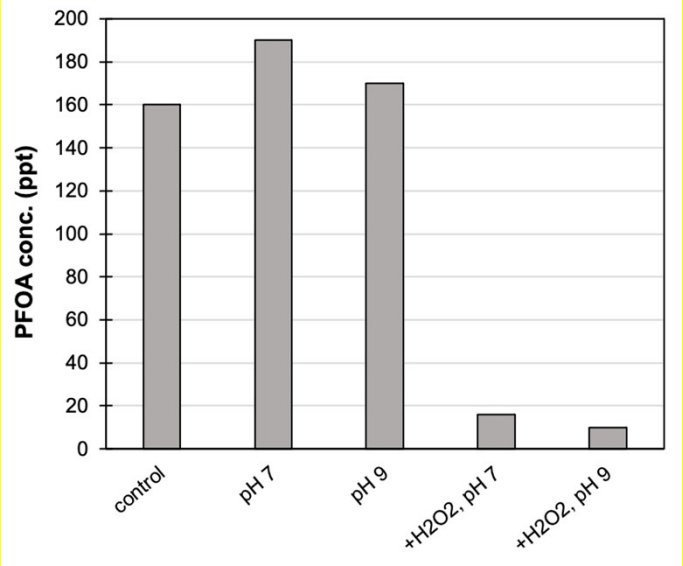


**Figure SF4.** PFOA concentrations in solutions with magnetite with and without added $H_2O_2$ and exposed to UV radiation. There is no significant change in PFOA concentration with magnetite particles suspended in the solution, compared to the control. Therefore, adsorption to magnetite is not a contributing factor to PFAS removal. In contrast, ROS generated when $H_2O_2$ is present in the solution result in a significant reduction in PFAS concentration.

## S3.3. XANES.

All samples were prepared with 1000 ppm $Fe_3O_4$ and underwent 30 min of UV-C exposure before analysis. Linear combination fitting results for these spectra are given in Table ST4. Analysis indicates no change in the peak energy of the K-edge (generally associated with oxidation state), disappearance or appearance of pre-edge or K-edge features, or intensity of these features. In all cases, the collected spectrum matches well with the $Fe_3O_4$ standard spectrum collected and shown in Figure SF3A. Further analysis by linear combination fitting (Table ST4) of 4 common Fe mineral spectra containing varied oxidation states of Fe emphasizes there is no change in the $Fe_3O_4$ after multiple reaction cycles. All samples are shown to be between 94-100% (estimated fit error ± 3%) $Fe_3O_4$ in their Fe bonding characteristics. There is one outlier in the 2.55M, pH9 sample

after one cycle, which shows only about 89% $Fe_3O_4$, and this outlier is likely due to difficulty in normalizing this specific spectrum, which may cause the fit to have a larger error.

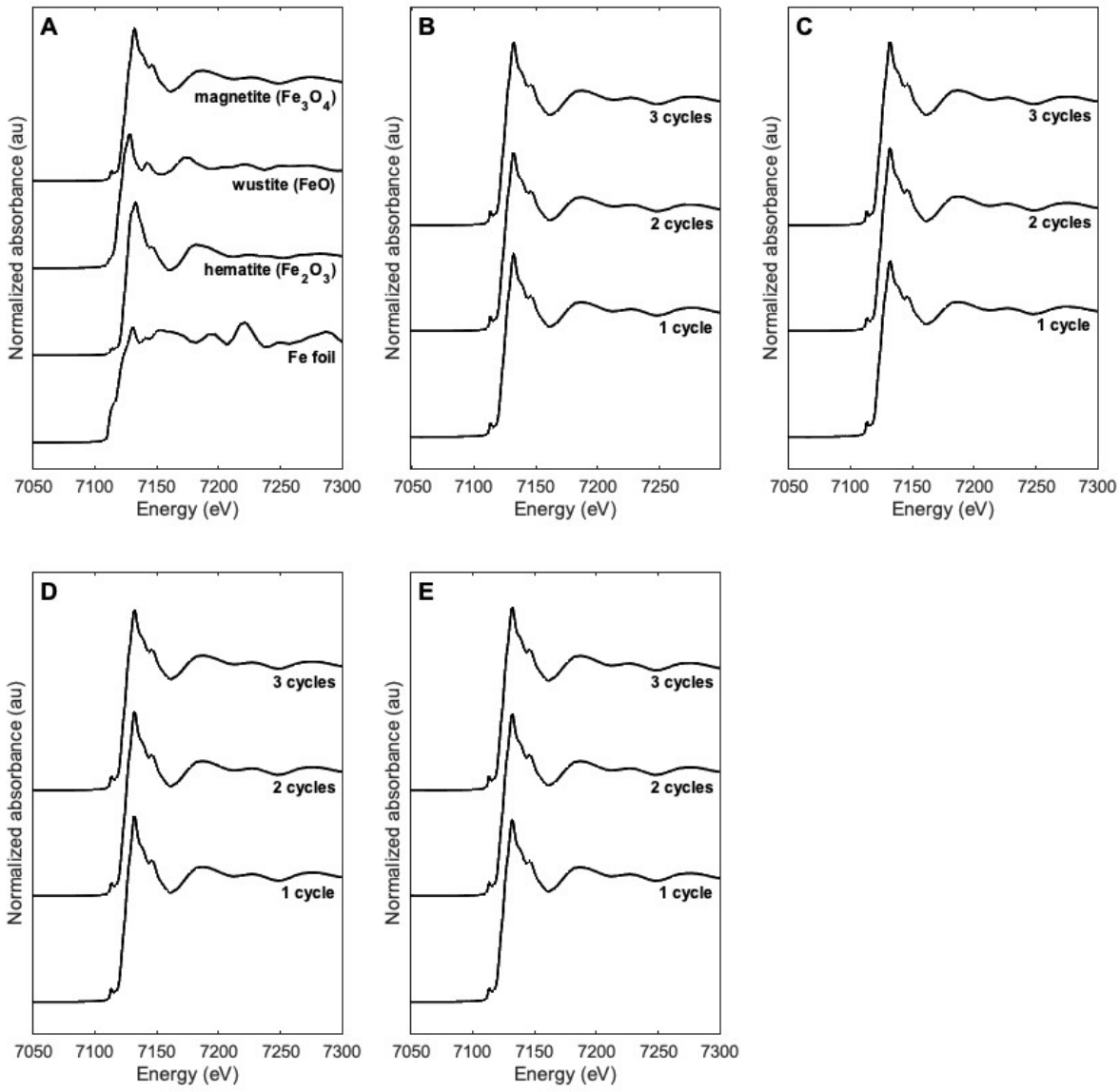


**Figure SF5.** Fe K-edge XANES spectra for Fe standards **(A)** and $Fe_3O_4$ NPs after variable number of UV-Fenton cycles and solution conditions: **(B)** 2.55 M $H_2O_2$, pH 7, **(C)** 2.55 M $H_2O_2$, pH 9, **(D)** 5 M $H_2O_2$, pH 7, **(E)** 5 M $H_2O_2$, pH 9.

**Table ST2.** Linear combination fitting of Fe K-edge XANES using four common Fe standards with varied Fe speciation and local bonding states. The reported R-factor represents the goodness-of-fit.

| Samples | Fe foil | $Fe_2O_3$ | FeO | $Fe_3O_4$ | R-factor |
|---|---|---|---|---|---|
| 2.55 M $H_2O_2$, pH 7 | | | | | |
| 1 cycle | 0.016 | 0 | 0.014 | 0.970 | 0.000055 |
| 2 cycles | 0.049 | 0 | 0.015 | 0.930 | 0.000325 |
| 3 cycles | 0.022 | 0 | 0.004 | 0.974 | 0.000068 |
| 2.55 M $H_2O_2$, pH 9 | | | | | |
| 1 cycle | 0.075 | 0 | 0.032 | 0.889 | 0.000633 |
| 2 cycles | 0.020 | 0 | 0.007 | 0.972 | 0.000054 |
| 3 cycles | 0.017 | 0 | 0.010 | 0.974 | 0.000044 |
| 5 M $H_2O_2$, pH 7 | | | | | |
| 1 cycle | 0.000 | 0 | 0.005 | 0.997 | 0.000007 |
| 2 cycles | 0.010 | 0 | 0.004 | 0.987 | 0.000025 |
| 3 cycles | 0.045 | 0 | 0.013 | 0.941 | 0.000242 |
| 5 M $H_2O_2$, pH 9 | | | | | |
| 1 cycle | 0.028 | 0 | 0.017 | 0.955 | 0.000094 |
| 2 cycles | 0.028 | 0 | 0.016 | 0.956 | 0.000112 |
| 3 cycles | 0.022 | 0 | 0.006 | 0.971 | 0.000059 |

## Supplementary References


(1) Trojanowicz, M.; Bobrowski, K.; Szostek, B.; Bojanowska-Czajka, A.; Szreder, T.; Bartoszewicz, I.; Kulisa, K. A Survey of Analytical Methods Employed for Monitoring of Advanced Oxidation/Reduction Processes for Decomposition of Selected Perfluorinated Environmental Pollutants. *Talanta* **2018**, *177* (September 2017), 122–141. https://doi.org/10.1016/j.talanta.2017.09.002.

(2) Yamamoto, T.; Noma, Y.; Sakai, S. I.; Shibata, Y. Photodegradation of Perfluorooctane Sulfonate by UV Irradiation in Water and Alkaline 2-Propanol. *Environ. Sci. Technol.* **2007**, *41* (16), 5660–5665. https://doi.org/10.1021/es0706504.